Microstructural and Metallurgical Characterization of Prematurely retired PT6A-114A High Pressure (HP) Compressor Turbine (CT) Blades used for Short-Haul Aircrafts

J. K. Ngoret and V. P. Kommula

Abstract—This paper presents microstructural and metallurgical characterization of prematurely retired from service high pressure (HP), PT6A-114A engine CT blades at 6378 creep-fatigue hours against a preset 10000 creep-fatigue hours. Sample preparation entailed; sectioning, mounting, grinding, polishing and carbon coating. A detailed microstructural and metallographic characterization was then performed on the prepared samples using x-ray florescence (XRF), x-ray diffraction (XRD) and scanning electron microscopy (SEM) on the material. The XRF results affirmed the existence of the bulk constituent elements that matched the manufacturers' specification. The XRD analyses enabled positive identification of the resultant compounds which constituted the protective coating and the substrate material. The SEM results established that the protective coating of the tips was more attacked compared to the airfoils and the bases and as a result, the substrate material equally degraded.

***Keywords*—**Inconel 713LC, x-ray florescence, x-ray diffraction, energy dispersive spectroscope-scanning electron microscopy.

I. Introduction

The accuracy of acquisition and interpretation of results for microstructural and metallurgical investigations is enhanced depending on the quality of specimen preparation [1, 2]. With the exceptional characteristics of high temperature Nickel base super alloys which include; chemical composition, microstructure, type of carbides, microporosity, and even surface texture [3-7], quality preparation of samples stands to offer superior results. For casted blades of Nickel based superalloys, for which the specimens in the study belong; grain size, orientation, morphology, spacing of ɤ' carbide phase, and matrix microstructure are key [8, 9].

II. Materials and Specimens

Polycrystalline Inconel 713LC Ni-base alloy was used in manufacture of the blades used in this study. The specimens presented in Fig. 1 were collected from Vector Aerospace Kenya Limited.

Figure 1: High Pressure (HP), PT6A-114A engine CT blades

The composition of the material is as captured in Table 1 below.

Table 1: Composition of Inconel 713LC [10, 11]

Ni	**Al**	**Cr**	**Ti**	**Mo**	**Fe**
74	6.1	12.5	0.8	4.2	-
C	**B**	**P**	**S**	**Nb**	**Zr**
0.05	0.012	0.006	0.004	2.1	0.1

III. Experimental Approach

The samples of the CT blades were treated to a number of procedures in conformity to ASTM E3-11 which entailed; sectioning, mounting, grinding, polishing and carbon coating.

a) Sectioning

The samples for both transverse and longitudinal sectionings were cleaned and marked as presented in Fig. 2 (a) and (b) respectively [12, 13] to enable identify the morphology, attacks, present, lost and intruder elements and their roles in premature failure of the protective coating and substrate material of the CT blades.

The transverse sections were carried out at intervals of 33.3%,66.7% and 83.3% from the root of the CT blades whose lengths are 36mm to give a fair representation of the base, airfoil and tip sections using aDace Technologies, Picco 155P precision cutter, in Fig. 3.

J. K. Ngoret,Department of Mechanical Engineering, UB &Department of Mechanical Engineering, JKUAT (Phone: +254726557186; e-mail: jngoret@jkuat.ac.ke).
V. P. Kommula, Department of Mechanical Engineering, UB(E-mail: kommula@mopipi.ub.bw).

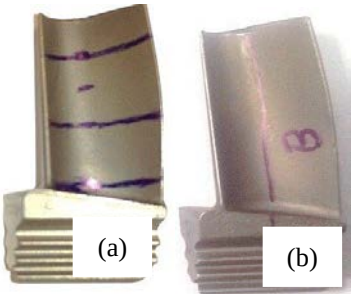

Figure 2: Marked samples for sectioning (a) Transverse (b) Longitudinal

Figure 3: Dace Technologies, Picco 155P, precision cutter

b) Mounting

Mounting was carried out in hot grey acrylic thermoplastic resin to preserve the edges and make recording of specimen details possible with the aid of StruersCito Press 30, mounting machine in Fig. 4.

Figure 4: StruersCito Press 30, hot compression mounting machine

c) Grinding and Polishing

StruersTegramin 30, automatic simultaneous grinder and polisher in Fig. 5 was used to yield superior flatness, preserve the edges and to clearly reveal the microstructure in Table 2 was adopted.

Figure 5: StruersTegramin 30, automatic grinder and polisher

Table 2: Grinding and polishing procedures

Procedure	Time (Sec.)	Force (N)	Surface
Step 1	180	40	MD Piano 500
Step 2	330	20	MD Piano 1200
Step 3	180	40	MD Largo $9_{\mu m}$ suspension
Step 4	180	30	MD Dac $3_{\mu m}$ (polishing)
Step 5	600	Gravity	Colloidal Silica on Vibratory Polisher GIGA-1200

d) Carbon Coating

Finally, Quorum Technologies, Q300T ES carbon-coater, in Fig. 6 was used to enhance signal and improve surface resolution of the sections at microscopic level prior to exposure to the EDS enabled SEM for micrography and element mapping. Literature suggests that carbon coating is sufficient for Ni-base alloys, while cost is significantly cut in comparison to gold coating.

Figure 6: Quorum Technologies, Q300T ES carbon-coater

IV. Results and Discussions

a) Prepared Samples

Figs. 7 and 8 illustrate the final prepared samples of the transverse sections at the tip, airfoil and base as well as the longitudinal section of the CT blades respectively ready for micrography.


ii)

Figure 7: Transverse sections (a) Tip (b) Airfoil (c) Base

Figure 8: Longitudinal section

b) XRF Analyses

The bulk constituent elements of both the protective coating and the substrate material of the CT blades and are compared against the manufacturer's original specifications in Table 3.

Table 3: % comparison between original composition of Inconel 713LC and XRF

	Ni	**Al**	**Co**	**Si**	**Cr**	**Ti**	**Mo**
Original	74	6.1	-	-	12.5	0.8	4.2
XRF	49.93	23.3	9.73	6.15	4.91	2.59	2.26
	Fe	**C**	**B**	**P**	**S**	**Nb**	**Zr**
Original	-	0.05	0.012	0.006	0.004	2.1	0.1
XRF	0.37	-	-	-	-	-	-

In conformity with the original material's composition, the bulk base elements; Ni, Al, Cr, Ti and Mo were positively identified. A number of other trace constituent elements such as Zr, Nb, C and B were however undetected, possibly from active replacement by more reactive elements. Intruder elements such as Co, Fe and Si similarly found their way into the spectrum, possibly from fuel constituents or flight.

The dynamics of decrease and increase of the constituent elements could have been as a result of position of the scanned surface in respect to heat exposure along the profile of the CT blades and the activity level of *NiAl* inward or outward diffusion of during service.

c) XRD Analyses

i) Protective Coating

Three compounds formed the bulk of the peaks in XRD analyses as summarized in Table 4. A compound of Aluminium, Chromium and Nickel, $Al_{0.67}Cr_{0.67}Ni_{0.67}$ was predominant at peaks 1, 4, 7, 8, 9 and 10. Molybdenum, Vanadium and Silicon compound, $Mo_3Si_2V_3$ matched peaks 3, 5, and 9. Titanium and Aluminium compound, Al_1Ti_3 matched peaks 2 and 6. The results confirmed presence of Al and Ni diffusion as well as the other alloy modifying elements Cr, Mo, V and Ti.

Fig. 9 reports on the XRD spectrum of the protective coating on which the ten peaks and their relative positions were identified and recorded in Table 4.

Table 4: XRD identified peaks, their positions and respective counts

Peak No.	**1**	**2**	**3**	**4**	**5**
Position *[^{0} 2Θ]*	30.86	39.41	41.84	44.45	45.99
Height (Counts)	213.2	219.0	1705.7	24025	2883.7
Peak No.	**6**	**7**	**8**	**9**	**10**
Position *[^{0} 2Θ]*	48.80	55.31	64.74	73.40	82.08
Height (Counts)	665.6	1108.9	404.0	243.4	6021.8

ii) Substrate Material

Two compounds predominantly formed the bulk of the peaks; a Chromium Nickel compound, Cr_3Ni_1 matching peaks 1, 3, 4. The other compound Molybdenum Carbide C_1Mo_1, with peaks 2 and 6 positively identifying with it. The constituent elements of these compounds form the bulk of the base and alloying materials in Inconel 713LC substrate material.

Fig. 10 reports on the XRD spectrum on which seven peaks and their relative positions were identified and recorded in Table 5.

Table 5: XRD identified peaks, their positions and respective counts

Peak No.	**1**	**2**	**3**	**4**
Position *[^{0} 2Θ]*	35.64	36.29	43.94	50.75
Height (Counts)	392.04	392.04	15725.16	2693.61
Peak No.	**5**	**6**	**7**	
Position *[^{0} 2Θ]*	63.32	74.98	91.08	
Height (Counts)	129.96	2981.16	2043.04	

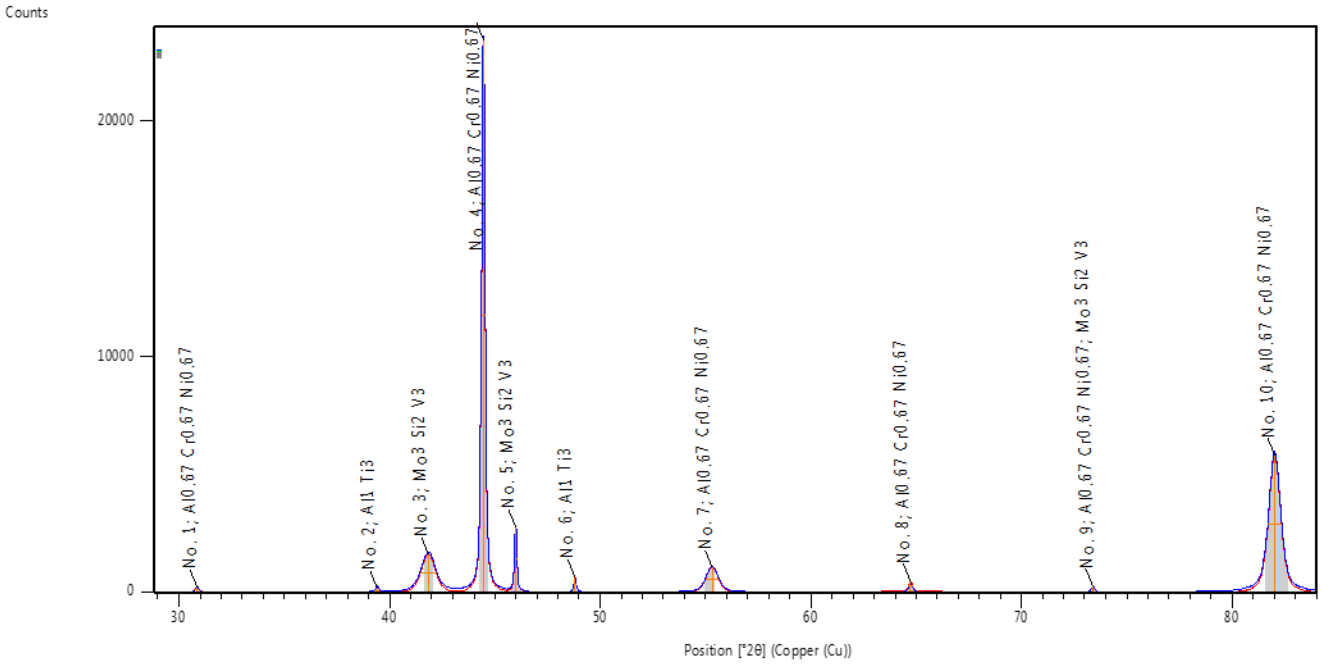

Figure 9: XRD spectrum of non-sectioned diffusive aluminide protective coating

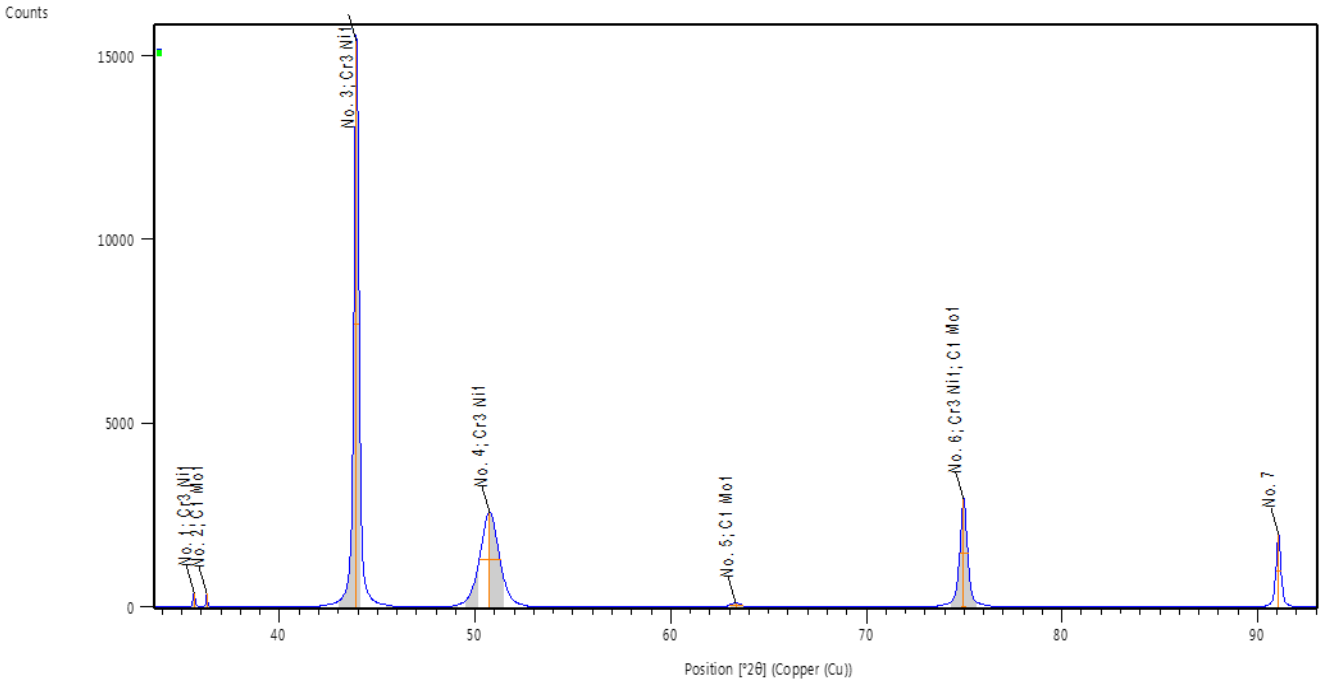

Figure 10: XRD spectrum of the sectioned substrate material

d) SEM Analyses

i) The Tip

The tip section had cracks originating from the protective coating and finding their way to the substrate material. Pores were evident and needles had developed as they appear in Fig. 11.

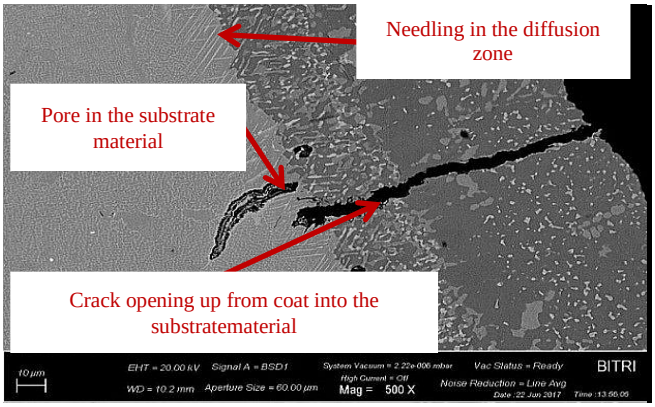

Figure 11: Sectioned tip

ii) The Airfoil

The micrograph in Fig. 12 presents evidence of pores with dispersions of white Ti MC carbides.

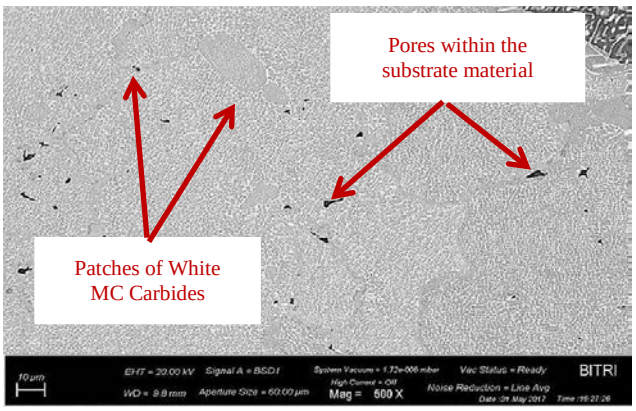

Figure 12: Sectioned airfoil

iii) The Base

Pores which are manufacturing defects could be identified at the base as shown in Fig. 13. However, contrary to presence of pores being thought to create potential weak points within the material, the base seemingly had a nearer uniform distribution of cuboidal phase as likened to the tip and airfoil. M_6C eutectic carbides were also noticed occasioned by slow heating up in this region, resulting in much longer heat retention, as such upon cooling, gradual precipitation is inevitable.

Dispersions of white MC carbides of Cr at the grain boundaries were evident from incomplete solutioning of the material as it ages.

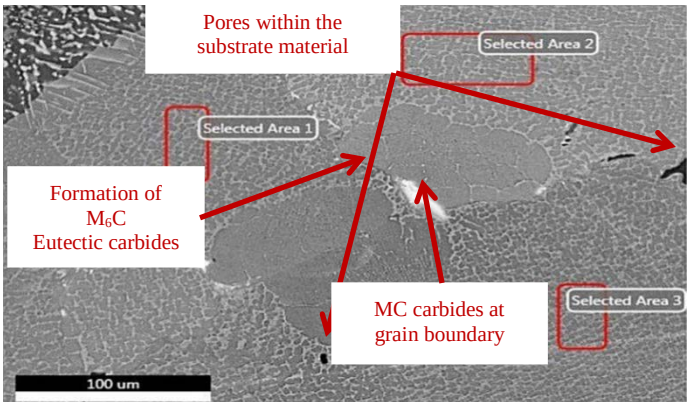

Figure 13: Sectioned base

V. CONCLUSION

This study sampled prematurely failed CT blades manufactured from Inconel 713LC for short-haul aircrafts in order to comprehend the magnitude of damage; they were exposed to before their premature. Sample preparation entailed; sectioning, mounting, grinding, polishing and carbon coating.

The samples were then treated to microstructural and metallographic characterization using XRF, XRD and SEM on the material. The XRF results confirmed the existence of the bulk constituent elements that matched the manufacturers' specification. The XRD analyses enabled positive identification of the resultant compounds which constituted the protective coating and the substrate material, while the SEM results established that the protective coating of the tips was more attacked compared to the airfoils and the bases and as a result, the substrate material equally degraded.The pores at the bases of the CT blades, which occur from manufacturing, were also found not influence distribution of uniform cuboidal phase of the substrate material.

ACKNOWLEDGEMENT

Appreciations go to The Office of Research and Development (ORD), University of Botswana (UB) for funding the research and Vector Aerospace Kenya Limited, for the samples and data collection from their premises.

REFERENCES

[1] V. Raghavan, Physical metallurgy: principles and practice: PHI Learning Pvt. Ltd., 2015.
[2] G. L. Kehl, The principles of metallographic laboratory practice: McGraw-Hill Book Company, 1949.
[3] C. Sims, The superalloys. New York, USA: John Wiley Pub., New York, 1972.
[4] J. Sieniawski, "Nickel and titanium alloys in aircraft turbine engines," Advances in Manufacturing Science and Technology, vol. 27, pp. 23-33, 2003.
[5] M. Zielińska, J. Sieniawski, and M. Poręba, "Microstructure and mechanical properties of high temperature creep resisting superalloy Rene 77 modified CoAl2O4," Archives of Materials Science and Engineering, vol. 28, pp. 629-632, 2007.

[6] M. Hetmańczyk, L. Swadźba, and B. Mendala, "Advanced materials and protective coatings in aero-engines application," Journal of Achievements in Materials and Manufacturing Engineering, vol. 24, pp. 372-381, 2007.
[7] A. Maciejny, "Development of high temperature creep resisting alloys," in Proceedings of the 1st Scientific International Conference „Achievements in Mechanical and Materials Engineering" AMME, 1992, pp. 32-36.
[8] G. Bell, P. Beeley, and R. Smart, "Tooling," Investment Casting, The Institute of Materials. Cambridge University Press, UK, pp. 40-41, 1995.
[9] S. Sajjadi and S. Zebarjad, "Effect of temperature on tensile fracture mechanisms of a Ni-base superalloy," Archives of Materials Science and Engineering, vol. 28, pp. 34-40, 2007.
[10] Nickel Institute. (2017, 25/05). Engineering Properties of ALLOY 713C [Media File]. Available: https://www.nickelinstitute.org/~/media/Files/TechnicalLiterature/Alloy713C_337_.ashx
[11] M. Zielińska, J. Sieniawski, M. Yavorska, and M. Motyka, "Influence of chemical composition of nickel-basedsuperalloy on the formation of aluminide coatings," Arch. Metall. Mat., vol. 56, pp. 193-197, 2011.
[12] S. Qu, C. Fu, C. Dong, J. Tian, and Z. Zhang, "Failure analysis of the 1st stage blades in gas turbine engine," Engineering Failure Analysis, vol. 32, pp. 292-303, 2013.
[13] L. Sexton, S. Lavin, G. Byrne, and A. Kennedy, "Laser cladding of aerospace materials," Journal of Materials Processing Technology, vol. 122, pp. 63-68, 2002.